Cent. Eur. J. Phys. • 11(4) • 2013 • 487-496
DOI: 10.2478/s11534-013-0211-7

VERSITA

Central European Journal of **Physics**

# A kinetic Monte Carlo study for stripe-like magnetic domains in ferrimagnetic thin films

**Research Article**

Botond Tyukodi[1], Ioan-Augustin Chioar[2], Zoltán Néda[1]*

1 *Babeş–Bolyai University, Department of Theoretical and Computational Physics Kogălniceanu street 1, 400084 Cluj-Napoca, Romania*

2 *Université Joseph Fourier, Domaine Universitaire 621 avenue Centrale, 38400 Saint-Martin-D'Héres, France*



**Received 24 August 2012; accepted 18 March 2013**

**Abstract:** The topology and dynamics of stripe-like magnetic domains obtained in a ferrimagnetic garnet subjected to a time-dependent external magnetic field is studied experimentally and theoretically. Experiments are performed on a commercially available magnetic bubble apparatus, allowing the observation of the time-evolution of the magnetic domain structure. The system is modeled by a meso-scale Ising-type lattice model. Exchange and dipolar interactions between the spins, and interaction of the spins with the external magnetic field are considered. The model is investigated by kinetic Monte Carlo simulations with time-varying transition rates. In the limit of low temperatures the elaborated model leads to a magnetic domain topology and dynamics that is similar to the ones observed in the experiments. In the highly non-equilibrium limit with a high driving frequency the model reproduces the experimentally recorded hysteresis loops as well.

**PACS (2008):** 75.70.Kw, 75.10.Hk, 75.60.Ej

**Keywords:** kinetic Monte Carlo • magnetic bubble • magnetic stripe domains • magnetic bubble apparatus



## 1. Introduction

Due to their potential applicability for information storage, the domain patterns with a striped morphology arising in magnetic thin films with a large crystalline anisotropy have been extensively investigated both experimentally and theoretically [1–4]. Theoretical modeling of such stripe domain patterns are usually performed following two main directions. The first possibility is by a continuum approach [5]. Studies in such direction consider a phenomenological description. The most well-known approach in this category is the nowadays fashionable micromagnetic simulations [6]. The second possibility is to use a micro- or mesoscopic approach with lattice-type models [7]. Both approaches have advantages and disadvantages as well. The former, while in general is capable to capture a larger variety of static and dynamic phenomena, has no direct connection to the microscopic structure of the material and the dynamics in such an approach is purely phenomenological. Also, such methods end up in solving complicated partial differential equations

*E-mail: zneda@phys.ubbcluj.ro

or integral equations [8, 9] with complex boundary conditions, increasing considerably the required computational effort. On the other hand, lattice models have the advantage that the characteristic Hamiltonian of the system incorporates the realistic interactions between the sites and the system can be easily studied by simple Monte Carlo (MC) type simulations. The dynamics implemented in such models are however also phenomenological ones, having no rigorous theoretical foundations. Various lattice models have been introduced so far, ranging from the Ising-type models involving long range coulombian interactions [12, 13] to the spin-glass type models with oscillating long range (RKKY-type) interactions [14]. Once an interaction scheme has been established, lattice models are usually investigated using either canonical [12] or microcanonical [15] MC methods. The finding that such models reproduce successfully the striped morphology is not surprising at all, since it has been recently proved that stripe patterns are a straightforward consequence of competing isotropic pairwise interactions [16]. The validity of such lattice models therefore cannot be concluded solely by the fact that they reproduce the right patterns under certain combinations of the external parameters. Another drawback of lattice models is that although they are based on microscopic elements and microscopic level interactions, they are in fact mesoscopic models. Indeed, in reality the width of the domains is of several orders of magnitude larger than the distance between two lattice sites, making impossible a realistic microscopic MC simulation due to the required huge lattice size. In lattice simulations usually a domain is composed of several spins only, meaning that a renormalized approach is considered, where one lattice site represents a mesoscopic element of the material. For a rigorous approach, a quantitative upscaling from the microscopic level to the mesoscopic one would be necessary in order to properly map the spin values and the interaction constants from the molecular level to our coarse-grained model. This mapping would definitely lead to a nonlinear rescaling of the temperature as well. One of the main problems with the lattice-type models is that such a rigorous scaling is not available so far, therefore, it is impossible to compare the model parameters and the simulation temperature with their experimental counter-values. Most of the previous attempts based on lattice models disregarded the fact that such models have to be interpreted on a mesoscopic level, and the fact that the model parameters are related by an unknown complex nonlinear mapping to the realistic values. As a consequence of this they considered simulation temperatures not too far from the critical one, without rescaling the temperature values according to the mesoscopic interpretation of the lattice models. A simple qualitative renormalization argument can convince us that the mesoscopic interpretation of the lattice model would require extremely low simulation temperatures (respective to the Curie temperature of the system), in order to realistically model the experimental system. Indeed, if one spin in the lattice represents a block-like magnetic domain, the interaction constants with the neighbours should be orders of magnitude higher than the real values, meaning that the ordering effect dominates the entropic one in the model. This naturally leads to the fact that in the mesoscopic lattice model an extremely small temperature value (in comparison with the critical one) has to be considered. Due to the fact that previous lattice model attempts were considered at temperatures much closer to the critical value, although the resulting patterns were similar to the experimental ones, the obtained time-evolution was wrong. Instead of nucleating several long stripes, dot-like patterns appeared which, in turn, were connected and finally the stripes emerged.

Due to the above discussed problems, momentarily we have no simple way to model realistically such systems. Our purpose here is to reconsider experimentally and theoretically the strip-like domain formation problem in magnetic thin-films, and beside the final equilibrium patterns to describe also the dynamics of the system in varying magnetic fields. For the experiments we use a student laboratory device, called *magnetic bubble apparatus*, which is commercially available[1]. Theoretically, we define a mesoscopic level lattice model and perform a rigorous low-temperature non-equilibrium Monte Carlo simulation on such systems, comparing the evolution of the stripe-like patterns in varying external magnetic field to those obtained from experiments. Since the considered system is out of equilibrium, a kinetic Monte Carlo method with time dependent transition rates is implemented.

## 2. Experimental method

The core of the experimental setup is the *magnetic bubble apparatus*, which is a standard device for student laboratories. In the middle of this device a ferrimagnetic garnet film is placed between two parallel polarizers having rotated planes of polarization with respect to each other. The chemical composition of the film is $Bi_{0.6}Tm_{2.4}Ga_{1.15}Fe_{3.85}O_{12}$ and it has a high crystalline anisotropy oriented perpendicularly to the plane of the film. Due to this high anisotropy, the magnetization is

[1] *http://www.telatomic.com/electricity/magnetic_bubble.html*

always perpendicular to the plane of the film and points either upwards or downwards. The magnetic domains that will form due to the competing exchange and dipolar interactions will have a strip-like structure with two possible orientations for the magnetization. The thickness of the film is about $8\mu m$, while its planar extent is of the order of millimeters. The garnet is surrounded by a solenoid and the external magnetic field experienced by the layer can be directly controlled through the current in the solenoid which is obtained from a signal generator. The experimental device is summarized in Figure 1.

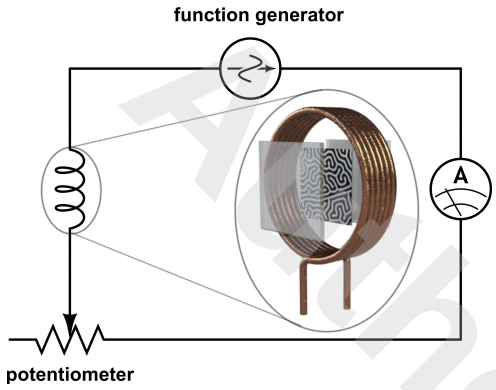


**Figure 1.** Sketch of the experimental setup and magnetic bubble apparatus.

When illuminated from the bottom, after passing the first polarizer the incoming light becomes plane polarized and experiences the two different magnetization directions of the domains. According to the Faraday-effect, the polarization plane of the light is rotated in different directions for different magnetizations. After passing the second polarizer, the intensities of the beams passing through the oppositely oriented domains will be different and as a result of this the domain structure becomes visible.

In the experiments a varying external magnetic field was created in the solenoid by using an amplified sine-wave signal with a large period ($\sim$ 20 minutes). Since the characteristic relaxation times in magnetic processes are of the order of nano- or microseconds, in the experiments, we definitely created equilibrium configurations for each magnetic field value. Although much larger driving frequencies would have done the job, due to the relatively large recording time of the microscope-camera (1 frame/second), we have chosen to work with a comfortable period value where we insured that all visually observable changes in the domain structure are recorded. An optical microscope with a CCD camera as objective was used to observe and record the time evolution of the magnetic domain structure. The recorded images were subjected to several image processing steps in order to obtain a clear black and white picture. The difficulties appeared from the fact that for various magnetization values the overall light intensity was different and the brightness was non homogeneous in the studied layer. As a result in a simple image analyses method different threshold values would have had to be chosen for the black and white conversion of different images. We have chosen instead a more sophisticated method which has the advantage that it applies for all the pictures. Due to the poor quality of the pictures, a noise reduction was applied as a first step. This was accomplished by the commercially available Photoshop software by setting the parameter "Strength" to 10 and all the other parameters to 0. For the next step, another software package, called *ReaConverter* was used, and a black and white conversion was applied to the images with a blur of radius 2.5 (pixels) using the "maximum entropy algorithm". Although the parameters of the image processing technique definitely affect the results, it has no effect on the qualitative description of the system. The finally obtained pictures offered a simple interpretation for the domain structure and allowed the extraction of the resulting total magnetization for the observed region. Magnetization was calculated simply as the difference between the black and white pixels in the picture. In Figure 2 we show both the originally recorded gray-scale image and the black and white image processed from this.

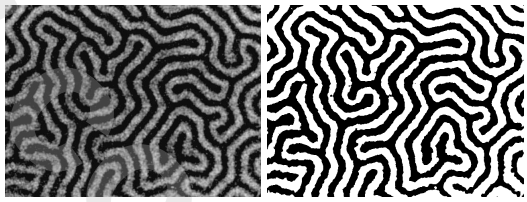

**Figure 2.** The figure on the left shows the originally recorded gray-scale image and the figure on the right is the processed black and white image.

The intensity of the current flowing through the solenoid was recorded by a digital ammeter. It was assumed that this current intensity is proportional to the intensity of the magnetic field created in the solenoid and applied on the ferrimagnetic garnet. Having information both on the magnetization of the sample and the relative intensity of the applied external magnetic field, it is possible to construct the experimental hysteresis curve. A characteristic hysteresis loop, together with some characteristic domain structures corresponding to different magnetic field values are presented in Figure 3. One will observe the following characteristic features: (1) shrinking of the hysteresis loop in the vicinity of small external fields; (2) after saturation, for nucleating inversely oriented domains a considerable change in the applied field is needed. From

the recorded domain structures we also learn how the domain structure is evolving when the magnetic field is increased in the opposite direction of a saturated magnetization. First, a line-like oppositely oriented domain nucleates. Increasing further the magnetic field in the direction of the nucleated domain will result in nucleating new branches and a concomitant folding and thickening of this line. After achieving a state where both domain orientations are equally probable, the domains with an opposite magnetization direction relative to the magnetic field are thinning up to a complex line-like structure, and collapse in clearly observable jumps. These jumps are also observable during the nucleation dynamics of the domains. Moreover, during the folding stage, a clear pinning-like behavior is observed: instead of smoothly winding up, the stripes move intermittently, a behavior caused by defects or impurities of the thin film and which, in turn, results in a non-vanishing equilibrium hysteresis. In Figure 3, we illustrate with a couple of experimentally recorded configurations the above described dynamics. One can observe that the hysteresis loop is non-symmetric relative to the $M = 0$, $B = 0$ center (biased in one magnetization direction), and it is also unexpectedly wide in this limit. This might be the influence of the substrate the ferrimagnetic layer was deposited on, however, more probably, it is an artifact of the binarization technique. Alternatively, the small field of view of the microscope can also bias our measurements. In order to address this issue, better quality images with bigger sample sizes and a more rigorous and better controlled binarization method is required. This issue has not been addressed within our simple experimental procedure.

Previous experiments have shown that the emerging stripe-like domain topology is not the only characteristic structure that can appear in such ferrimagnetic films. It is possible to observe other structures (bubbles or a foam-type pattern) using different experimental conditions (temperature, external magnetic field). The equilibrium domain structure actually depends also on the annealing history of the system, whether it was cooled fast or slowly, or in zero or non-zero external field [2, 10, 11]. Nevertheless, the present study focuses only on the investigation of the stripe-like labyrinth patterns that are revealed by the magnetic bubble apparatus at room temperature.

## 3. Theoretical model

Due to the high perpendicular crystalline anisotropy of the ferrimagnetic garnet, the magnetization is always perpendicular to the plane of the film and the magnetization of the domains can have only two oppositely oriented directions. It is therefore reasonable to consider a lattice model with Ising-type spins that can take values $S_i \in \{\pm 1\}$. As it was already emphasized in the Introduction, in such an approach one spin will model a mesoscopic element of the garnet.

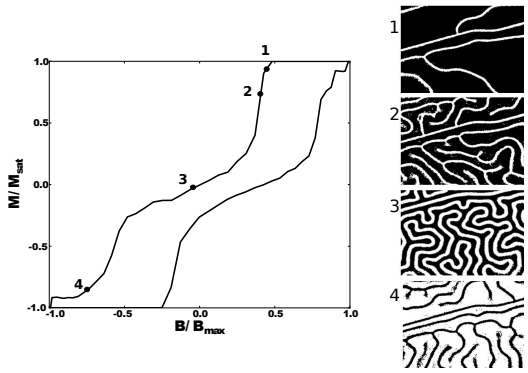


**Figure 3.** Experimental hysteresis loop (left) and the processed black and white domain structures corresponding to the indicated points.

In a simple lattice model for this magnetic system the ferromagnetic ordering within the domains appears as a result of an Ising-type exchange interaction. In order to obtain oppositely oriented magnetic domains, a long-range dipolar magnetic interaction should also be included. Since we intend to study also the effect of an external magnetic field, the Hamiltonian of the system must contain a term that describes the interaction of the spins magnetic moments with the external magnetic field. In conclusion, the simplest Hamiltonian for the system writes as:

$$H = -J \sum_{\langle i,j \rangle} S_i S_j + D \sum_{\{i,j\}} \frac{S_i S_j}{r_{ij}^3} - B \sum_{\{i\}} S_i. \qquad (1)$$

The first term corresponds to the exchange interaction, and here the sum is for all nearest neighbour spin pairs. The second term describes the magnetic dipolar interaction, and the sum in this term refers to all possible spin pairs in the system (neglecting of course the $i = j$ situations). It is worth mentioning here that according to the considered geometry (spin orientations perpendicular to the plane of the film), in this term we have omitted the obviously null contributions. The last term describes the magnetic interaction of the spins with the external magnetic field. Due to the two allowed spin orientations, there is no need for vectorial notations, the algebraic values will do the job. The same Hamiltonian has already been used in previous works ([12, 13] for instance). The model as it is written in equation 1 has two independent parameters: $J$ and $D$. In case one needs to investigate thermodynamic quantities, the system's temperature, $T$, will also be a free parameter.

Let us first make more quantitative the mesoscopic interpretation of this simple spin model. Figure 4 shows how the relevant microscopic quantities scale while moving from individual spins to a coarse-grained, mesoscopic interpretation. In the illustrated coarse-graining step blocks of $N \times N$ spins are grouped and coupled with the rescaled $N \cdot J$ exchange interactions. Summarizing, the following quantitative scaling is performed: $S \to N^2 S$, $J \to NJ$, $D \to D$. The critical temperature resulting from the classical Ising model (in case of $D = 0$), $T_c = JS^2 q/3k$ ($q$ is the number of first order neighbours on the lattice), scales as: $T_c \to N^5 T_c$. In order to have mesoscopic block sizes, $N$ must be large. This means that if we intend to understand the system's behavior below the critical temperature, in the mesoscopicaly interpreted model one has to consider extremely low temperatures relative to the critical one, since the critical temperature is upscaled by an $N^5$ factor.

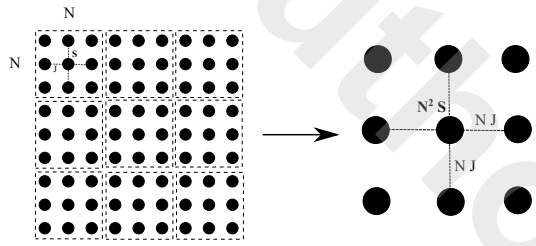


**Figure 4.** Quantitative up-scaling to the mesoscopic approach.

Considering $J > 0$ and $D > 0$ values, it can be readily foreseen that a competition between the exchange and dipolar interaction arises, resulting in a characteristic domain structure. In order to improve the isotropy of the domain configurations, the model is implemented on a triangular lattice.

## 4. Simulation method

The structure and dynamics of the magnetic domains are investigated through the lattice model defined by the Hamiltonian (1) considering magnetic fields varying in time and low temperature conditions. Due to the fact that we simulate the model at temperatures much smaller than the critical one, a kinetic Monte Carlo (kMC) method is implemented.

The kMC method (or sometimes labeled as BKL Monte Carlo method [17]) has been developed for studying lattice models at low temperatures or for investigating dynamical phenomena where the transition rates can take widely different values, depending on the system's actual configuration.

In its original form [17] it has been considered for equilibrium problems where the transition rates are time independent. The main idea of the method is that in each simulation step one possible transition is carried out, and the time is updated non-uniformly, according to a theoretically justified recipe.

When simulating systems at low temperatures, the Metropolis and Glauber dynamics are extremely inefficient. Both methods are of acceptance-rejection type, i.e. in each simulation step a new configuration is either accepted or rejected, and the acceptance rate decreases rapidly with the temperature. In the Metropolis algorithm, for instance, the probability of accepting a new state if its energy is higher than the actual state's energy is $\exp(-\Delta E/kT)$. This means that at low temperatures it is almost impossible for the system to escape from the local potential well and to proceed towards the global equilibrium. Obviously, all the rejected states are realistically part of the dynamics and they should be taken into account when computing averages of various quantities, however, they do not help in evolving the system ahead in time. The kMC method was originally introduced in order to overcome this "freezing" issue at low temperatures. The main idea is to carry out a transition in each simulation step, and fuse all the rejected transitions together by computing a realistic "waiting" time between two accepted events. Once this idle time is computed, one possible transition is selected and carried out and the time is updated. Let us denote by $r_i$ the Metropolis (or Glauber) transition rates of the possible transitions that are labeled here by $i$. These $r_i$ values are in fact the probabilities that transition $i$ occurs in unit time. Also, let us denote by $R = \sum_i r_i$ the cumulative transition rate. In the kMC scheme in each simulation step, one of the transitions is carried out with a probability proportional to its transition rate $r_i$.

Let us now show how to update the simulation time properly. If the time interval from the last accepted transition (occurring at time moment $t_0$) till the the next event (occurring at time $t_0 + \tau$) is divided into infinitesimally small $dt$ intervals, the probability that transition $i$ occurs within one of these $dt$ intervals is $r_i dt$. Then, the probability that transition $i$ will not occur within the time interval $\tau$ is

$$P_i(\tau) = (1 - r_i\ dt)^{\tau/dt}, \tag{2}$$

which, in the limit of $dt \to 0$ leads to:

$$P_i(\tau) = \exp(-r_i \tau). \tag{3}$$

Now the probability that none of the possible transitions occurs within this $\tau$ interval is:

$$P(\tau) = \prod_i P_i(\tau) = \exp\left(-\sum_i r_i \tau\right) = \exp(-R\tau). \quad (4)$$

The probability that a transition occurs within the next $dt$ interval after a $\tau$ waiting time is

$$P_{tr}(\tau) = \frac{d[1 - P(\tau)]}{d\tau} dt = R \exp(-R\tau) dt, \quad (5)$$

meaning that in order to obtain the proper $\tau$ waiting times, they have to be generated according to the 5 distribution. It is easy to prove that this can be accomplished by generating a uniform random number $u \in [0, 1)$ and computing a probabilistic waiting time as:

$$\tau = -\frac{\ln u}{R}. \quad (6)$$

In the problem considered here the magnetic domains evolve in a varying external field, so we deal with a non-equilibrium situation. As a result of this the transition rates used for the kMC algorithm are time-dependent ones. Instead of the usual kMC algorithm, we use a method described in reference [18], which is appropriate for non-equilibrium systems with time-dependent transition rates: $r_i = r_i(t)$. In this approach, the probability that transition $i$ will not occur up to a time interval $\tau$ measured from the last transition is:

$$P_i(\tau) = \prod_k (1 - r_i(t_k) dt) \approx \prod_k \exp[-r_i(t_k) dt], \quad (7)$$

where $t_k = t_0 + k dt$. In the continuum limit:

$$P_i(\tau) = \exp\left(-\int_{t_0}^{t_0+\tau} r_i(t) dt\right), \quad (8)$$

and the probability that none of the transitions will occur writes as:

$$P(\tau) = \exp\left(-\int_{t_0}^{t_0+\tau} R(t) dt\right). \quad (9)$$

The probability that transition will occur exactly within the $[t_0 + \tau, t_0 + \tau + dt]$ interval is:

$$P_{tr}(t_0 + \tau) = \frac{d[1 - P(t_0 + \tau)]}{d\tau} dt = R(t_0 + \tau) \exp\left(-\int_{t_0}^{t_0+\tau} R(t) dt\right) dt. \quad (10)$$

Consequently, the transition times $\tau$ with the distribution given by eq. (10) are obtained from the equation

$$-\ln u = \int_{t_0}^{t_0+\tau} R(t) dt; \quad (11)$$

where $u \in [0, 1)$ is a uniform random number and $R(t) = \sum_i r_i(t)$ is the cumulative transition rate (for a thorough and comprehensive description of the method, see reference [18]). For speeding up the simulations it is desirable to evaluate with minimal numerical calculations the individual transition rates. In order to do that we have written the individual transition rates $r_i$ (i.e. the rate of flipping spin $i$) as

$$r_i = \exp\left(-\frac{\Delta U_{flip}}{2kT}\right), \quad (12)$$

where $\Delta U_{flip}$ is the energy necessary to flip spin $i$. These rates, while satisfying the detailed balance in equilibrium, are symmetric to the back-and-forth transitions, and, due to the quantized energies in the system they are also bounded, hence no additional criteria are required. More importantly, these transition rates factorize into a time-dependent and time-independent part:

$$r_i = \exp\left(-\frac{\Delta(U_{\text{exchange}} + U_{\text{dipolar}})}{2kT}\right) \exp\left(-\frac{\Delta U_{\text{magnetic}}(t)}{2kT}\right). \quad (13)$$

It is easy to observe that only the second term (resulting from the interaction with the varying external field) is time dependent, and it has two possible values for the two spin orientations. The good news is that for a given spin configuration, the integral (11) can be evaluated now without calculating the sum $R(t) = \sum_i r_i(t)$ for each iterative time step, and this considerably reduces the needed simulation time.

The kMC method described in [18] was thus implemented with the above mentioned simplification. As it was discussed earlier, in order to get a better isotropy a triangular lattice of size $128 \times 128$ was used, and in order to reduce finite-size effects periodic boundary conditions were imposed.

## 5. Simulation Results

Our kMC simulations are aimed to reproduce the experimental conditions and results. A sinusoidally varying external magnetic field with a period of $2\pi \times 10^3$ time-units was imposed. In order to establish a connection with real experimental time-scales the time-unit for the kMC simulations should be interpreted in comparison with the

characteristic relaxation time. If one considers a system of spins with saturated magnetization (all spins pointing in the same direction) in zero magnetic field, the half-time for decay to the equilibrium state (stripped domain structure) with zero magnetization would be of 5 time units in the kMC simulations. Unfortunately, we do not have information on the experimental time-scale for the magnetic relaxation in our sample. We believe however that the maximum value of the characteristic relaxation time should be of the order of micro-seconds. This means that our simulation conditions would correspond with an experiment realized with a sinusoidally varying external magnetic field having a period of the order of milliseconds. This is orders of magnitude smaller than the one considered in our experiments meaning that the simulations are performed with a much higher frequency driving than the experiments. Increasing however the value of this driving period will result in the narrowing of the hysteresis loops, so we have chosen to perform the simulations with this high frequency external driving, and comment the conclusions later (see the Conclusions part).

Following the arguments presented in the introductory sections 1 and 3, the temperature was chosen very small: $T = 0.05T_c$, where $T_c$ would be the critical temperature of the pure Ising model with only nearest neighbour exchange interactions on the two-dimensional triangular lattice. The other parameters of the model are fixed as: $J = 1.0$, $D = 0.5$ and $B_{max} = 2.0$. All these values have the dimension of energy, and are given in the units fixed by the Boltzmann constant as $k = 1$.

In order to facilitate the nucleation of the first domain in a saturated sample, we have always introduced one nucleation center composed of a single spin pointing into the opposite direction of the saturated magnetization. The reason for doing this is to introduce an inhomogeneity in the system. Since periodic boundary conditions were imposed, all spins in the system have an identical neighbourhood and they are in a deep potential well at saturation. Therefore, when lowering the external magnetic field, spins start flipping at very different, sometimes even reversed orientation of the external field. In real systems this behavior will not occur due to the presence of some special spins that can change orientation easily. These spins are either in the neighbourhood of some inhomogeneity or at the edge of the sample, and will act thus as nucleation centers. We have reproduced these easy nucleation centers by the inversely oriented spin.

Performing the kMC simulations, for zero magnetic field, we obtained the characteristic strip-like domain patterns (Figure 5) which are qualitatively similar with the ones recorded in the experiments (Figure 2).

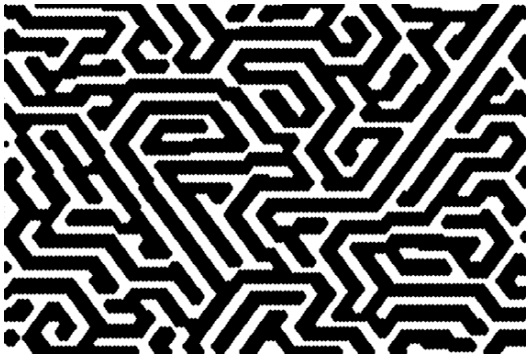

**Figure 5.** Strip-like domain patterns obtained by the kMC simulations at zero external magnetic field.

In order to be a little more quantitative in comparing the experimental and simulated domain structures we looked for some relevant numerical measures. Considering the most obvious method, a simple Fourier transform of the domain structures, will not yield the required numerical accuracy for distinguishing between various domain topologies in the plane. Instead, we found that by considering the diffusion of fictitious particles through these domain structures will give accurate enough statistical informations to characterize the topology of the strip-like domains. Our method can be briefly described as follows: (1) we chose one type of domain (either the "black" or the "white" one) and start random walkers on the selected domain; (2) the trail of the walkers are limited by the domain boundaries; (3) their average distance from the starting point as a function of simulation time will characterize the topology of the labyrinth they walk on. The starting points for the walkers were chosen from the middle part of the pictures and the pictures were scaled such that the average domain sizes from the experiments and simulations to be of the same sizes in pixels. The total sizes of the pictures in pixels were also the same. The walkers were always bounced back from the edge of the picture and domain boundaries, meaning that their number was conserved. Consequently, after sufficiently long time, an equilibrium average distance is reached. Both the average equilibrium distance and the way it is reached as a function of time are a characteristic property of a given structure.

In order to get a rough picture about how suitable such a method is in characterizing the domain topologies, several artificially built structures were also considered. The average squared distance of the walkers as a function of time, obtained for the diffusion on the domain structures obtained from experiments and simulations, as well as on artificial structures like a single stripe, a spiral, a random stripe or a simple square box, are presented in Fig. 6.

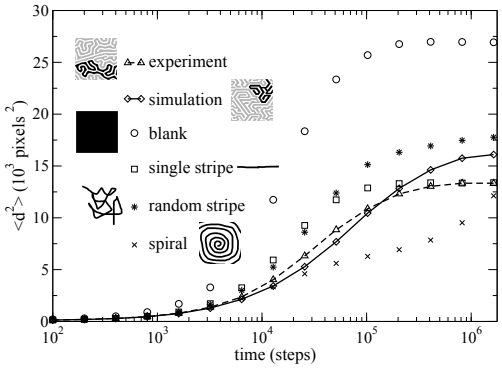


**Figure 6.** Averaged square distance of the random walkers as a function of simulation time on various diffusion channel topologies. For the details of the statistics see the text.

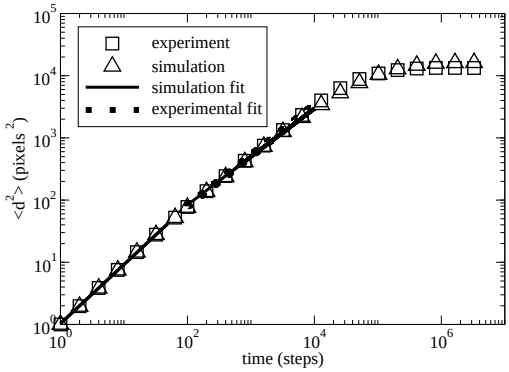


**Figure 7.** Quantitative comparison between the experimentally and theoretically obtained "labyrinth" structure of the domains through the scaling properties of the random walk. The averaged square distance of the random walkers as a function of simulation time is plotted on a log-log scale. Scaling exponents obtained from the two data are undistinguishable at this scale.

The time-unit is defined by the time needed for one step of the random walker, i.e. the time needed to jump to a randomly selected neighbouring pixel. The studied or artificially created diffusion channels were placed inside a square-like domain (illustrated in the legend of Fig. 6) of sizes 381 × 381 pixels. The results plotted in Fig. 6 are averaged on a number of $10^3$ trial starting points and for each starting point an ensemble average for $10^2$ walkers was performed. One can immediately see from the figure, that the method is suitable to distinguish between different domain topologies. As expected, the domain structures obtained in experiments and simulations, prove to be clearly distinguishable and quite similar in the view of the statistics obtained from diffusion. This becomes more evident by considering a logarithmic scale (Fig. 7). It can be readily observed that the statistics of the diffusion on both the experimental and simulated domain structure will exhibit three clearly distinguishable scaling regions. The first region corresponds to $t \in [1, 50]$. The explanation for the scaling here is simple: the average domain width in our pictures was of 14 pixels, so up to a square distance of about $(14/2)^2 = 49$ (corresponding to an average time of 49 units) an unrestricted, two-dimensional random walk takes place, where $\langle d^2 \rangle(t) = \alpha t^\beta$, with $\beta = 1$. Accordingly, both the experimental and simulated domain structures yield in this region a scaling exponent close to 1: $\beta = 0.95$ for the experiments and $\beta = 1.03$ for the simulations . The second region in Fig. 7, for $t \in [10^2, 10^4]$ suggests again a clear scaling with exponents that are smaller from the ones obtained in the first region. The best fit indicates $\beta = 0.81$ for the experiments and $\beta = 0.78$ for simulations (indistinguishable on the graph). This region describes the bending structure of the domains, and corresponds to length scales from 14 up to an average distance of 100 pixels, i.e roughly 1/3 of the presented image sizes. The similar scaling exponents suggests that the structures on this length-scales are statistically similar ones. The last region of the graph in Fig. 7, for ($t > 10^4$) shows the break-down of the scaling in both structures. Although on the logarithmic scale the differences between the experimental and simulated structures are not observable, one can see in Fig. 6 that they converge to different limits. This suggests that the structures are distinguishably different for length scales bigger that 100 pixels. An attentive comparison between the experimental and simulated domain structures will convince us, that the experimental domains are indeed longer than the simulated ones. This difference is quantified by the different convergence limits observable in Fig. 6.

The hysteresis loop obtained with the mentioned simulation parameters is plotted in Figure 8. Similarly with the experimental results, on this loop we indicate the characteristic domain structures corresponding to different external magnetic field values. Comparing the results with the experimental ones plotted in Figure 3 one will observe that the domain structure, their nucleation and dynamics are similar to the experimental one. Although the period of the imposed external magnetic field is much larger than the relaxation time of the system, the hysteresis loop is present and has a similar shape with the experimental one (Figure 3). We remind however, that this hysteresis is a consequence of the non-equilibrium dynamics and the loop becomes narrower as the period of the external field is increased in the kMC simulations. Despite the fact that at

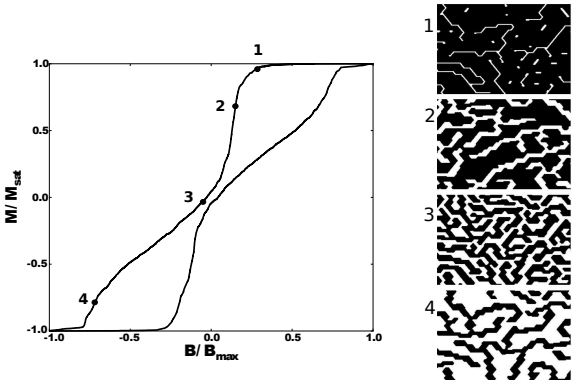


**Figure 8.** The hysteresis loop obtained by kMC simulations (left) and the characteristic domain structures corresponding to the indicated points.

the beginning of the simulation we impose a single nucleation center, on the simulated domain dynamics (Figure 8) multiple regions with reversed magnetization are observable. The appearance of these secondary nucleation centers are however a direct consequence of the induced nucleation and the long-range dipolar interaction. Without the initially introduced nucleation center they would not appear, and the dynamics of the magnetization reversal would be largely delayed and realized in an explosive manner.

Finally, let us consider a few remarks on the influence of the model parameters. Fixing the value of $J$ and increasing the value of $D$ leads to thinner domain strips, hence smaller spatial period of the patterns. Smaller $B_{max}$ values prevent reaching the saturation in magnetization, and higher values will increase the plateau at saturation. Higher simulation temperatures will result in domain nucleation dynamics and domain structures which are not in agreement with the experimental observations. Smaller temperatures would result both in numerical difficulties in the calculations and an increased simulation time. By increasing the period of the applied external magnetic field, the hysteresis loop gets unrealistically thin.

## 6. Conclusions

Domain structures and hysteresis in a ferrimagnetic thin film with high crystalline anisotropy, subjected to periodically varying external magnetic field was investigated. Experiments performed on a magnetic bubble apparatus gave precious information on the nucleation, structure and dynamics of the strip-like domains. By an appropriate image analyses method the experimental hysteresis curve was extracted. Theoretically the system was modeled using the simplest possible meso-scale lattice model. In such view the spins of the considered model correspond to mesoscopic elements of the magnetic film. Due to the high crystalline anisotropy of the investigated system a simple Ising spin-like model extended with a long-range dipolar interaction term was considered. We argued that in order to realistically model the experimental conditions, the system has to be considered at low temperatures. As a result of this, the model was investigated with a kMC type computer simulation method. Due to the time-evolution of the external magnetic field, we had to deal with time-varying transition rates, and this required a special implementation for the kMC method.

It was found that the model is successful in reproducing the experimentally observed hysteresis loop for the magnetization and the structure, nucleation and dynamics of the strip-like magnetic domains are also realistic. However, in order to succeed, it needs both a low temperature for the heat-bath and a high frequency for the external magnetic field. While the required low temperature condition is understandable from the viewpoint of the mesoscopic interpretation of the model, the relatively high frequency suggests that the model works well only in the highly non-equilibrium limit. If the experimentally considered quasi-equilibrium situation with a low driving frequency is considered, the model fails to reproduce the right shape of the hysteresis curve. Consequently, the magnetization value at remanence in this case is defined solely by the driving frequency of the external magnetic field, suggesting that the remanent magnetization is a dynamic effect. This is in contradiction with the experiments that suggest this is an equilibrium property of the film. The results indicate that the competing trend between the dipolar and exchange interactions is not enough to obtain enough magnetic frustration in the system. This is the main reason why many previous studies considered additional spin-glass like interactions, adding an extra frustration in the lattice model approach. Concerning the experiments we have to be cautious however, since as it was discussed in the section devoted to the experimental method, our method might be biased both by the considered small sample size and the used image processing method.

We conclude thus, that a minimal model, based only on exchange and dipolar interactions can offer a reasonable description for the obtained domain structures and their dynamics, assuming that a highly non-equilibrium simulation is done for the quasi-equilibrium experimental conditions.

## Acknowledgment

Work supported by the Romanian Complex Ideas research grant No. PNII/PCCE 312/2008. B. Tyukodi acknowledges the support of Collegium Talentum from Hungary. We thank I. Kézsmárki for providing us the magnetic bubble apparatus. We acknowledge the help of Zs. Vincze-Jankó in the preparation of Figure 1.

## References

[1] P. Molho, M. P. de Albuquerque, J. Magn. Magn. Mater. 226, 1388 (2001)
[2] M. P. de Albuquerque, P. Molho, J. Magn. Magn. Mater. 113, 132 (1992)
[3] M. Seul, L. R. Monar, L. O'Gorman, R. Wolfe, Science 254, 1616 (1991)
[4] P. Molho, J. Gouzerh, J. C. S. Levy, J. L. Porteseil, J. Magn. Magn. Mater. 857, 54 (1986)
[5] A. Kashuba, V. Pokrovsky, Phys. Rev. B 48, 14, 10335 (1993)
[6] J. Fidler, T. Schrefl, J. Phys. D: Appl. Phys 33, R135 (2000)
[7] E. Manousakis, Rev. Mod. Phys. 63, 1 (1991)
[8] A. Benassi, S. Zapperi, Phys. Rev. B 84, 214441 (2011)
[9] E. A. Jagla, Phys. Rev. E 70, 046204 (2004)
[10] S. R. Bakaul, W. Lin, T. Wu Appl. Phys. Lett. 99, 042503 (2011)
[11] M. W. Gutowski, K. Piotrowski, M. U. Gutowska, A. Szewczyk J. Magn. Magn. Mater. 242, 772 (2002)
[12] L. C. Sampaio, M. P. de Albuquerque, F. S. de Menezes, Phys. Rev. B 54, 6465 (1996)
[13] F. S. de Menezes, L. C. Sampaio Phys. Rev. B 72, 104413 (2005)
[14] J. R. Iglesias, S. Gonçalves, O. A. Nagel, M. Kiwi, J. Magn. Magn. Mater. 226-230, 548 (2001)
[15] A. D. Stoycheva, S. J. Singer, Phys. Rev. Lett. 84, 4657 (2000)
[16] E. Edlund, M. N. Jacobi, Phys. Rev. Lett. 105, 137203 (2010)
[17] A. Bortz, M. Kalos, J. Lebowitz, J. Comput. Phys. 17, 10 (1975)
[18] A. Prados, J. J. Brey, B. Sanchez-Rey, J. Stat. Phys. 89, 709 (1997)